60) 金子清俊: アメリカ産牛肉の輸入再開に関する公開討論会. 日本消費者連盟シンポジウム. 東京, 7.26, 2005

61) 金子清俊: 牛海綿状脳症 (BSE) と人変異型クロイツフェルト・ヤコブ病. 滋賀血液・免疫研究会. 滋賀, 7.30, 2005

62) 金子清俊: 牛海綿状脳症 (BSE) と人変異型クロイツフェルト・ヤコブ病. 夏期学校給食学習会. 横浜, 8.4, 2005

63) 金子清俊: 牛海綿状脳症 (BSE) と人変異型クロイツフェルト・ヤコブ病. 第二回柏崎認知症フォーラム. 新潟, 10.7, 2005

64) 八谷如美, 渡邉光太, 逆瀬川裕二, 金子清俊: Prion protein with Y145STOP mutation induces mitochondris-mediated apoptosis and PrP-containing deposits in vitro. 第 78 回日本生化学会大会. 神戸, 10.19-22, 2005

65) 八谷如美, 大久保卓哉, 小塚芳道, 逆瀬川裕二, 金子清俊: Over a hundredfold increase in immunoblotsignals of laser-microdissected inclusion bodies with an excessive aggregation property by Unfoldin/oligomeric Aip2p.第 78 回日本生化学会大会. 神戸, 10.19-22, 2005

66) 金子清俊: 牛海綿状脳症 (BSE) と人変異型クロイツフェルト・ヤコブ病. 第 12 回徳島神経難病治療薬研究会. 徳島, 10.28, 2005

67) 大西悠亮, 徳永勝士,金子清俊, 北條浩彦: 対立遺伝子特異的 RNAi 効果をヘテロ接合体下で評価するアッセイ系の確立. 第 28 回日本分子生物学会. 福岡, 12.5, 2005

68) 金子清俊: プリオンと蛋白質凝集. 平成 17 年度新潟大学脳研究所神経内科同窓会懇話会 40 周年記念講演会. 新潟, 11.19, 2005

69) 金子清俊: 変異型クロイツフェルト・ヤコブ病と牛海綿状脳症. プリオン病のサーベイランスと対策に関する全国担当者会議. 東京, 2.24, 2006

70) 金子清俊: あらためて BSE 問題を考える. 第 163 回情報懇話会 (連合通信社). 東京, 4.24, 2006

71) 金子清俊: 米国産牛輸入再開. BSE 緊急講演会 (生活協同組合東京マイコープ・パルシステム生活共同組合連合会). 東京, 5.18, 2006

72) 金子清俊: BSE に関する日本の実情. 健康権実現のための保健医療連合会公聴会. ソウル大学, 6.16, 2006

73) 金子清俊: 米国産輸入再々開. 第 2 回食の安全学習会. 大宮, 7.11, 2006

74) 金子清俊: 牛海綿状脳症 (BSE) と人変異型クロイツフェルト・ヤコブ病. 第 21 二回上越臨床神経懇話会. 新潟, 8.4, 2006

75) 金子清俊: アメリカ産牛肉輸入再開と BSE 問題. 岩手県消団連、いわて生協共催, 盛岡, 9.27, 2006

76) 金子清俊: BSE に関するフォーラム -アメリカ産牛肉の輸入再開-. 全国食健連, 東京, 11.11, 2006

77) 金子清俊. BSE と米国産牛肉の危険性について考える学習会. 全国農団労 ; 富山県農協労,富山, 12.19, 2006

78) 今川美登里, 八谷如美, 小見和也, 小塚芳道, 金子清俊: 培養細胞における正常型プリオン蛋白質の挙動 – GFP 融合蛋白質安定発現株での輸送速度及び siRNA による発現阻害効果の検討について -. 2006 年プリオン研究会. 盛岡, 9.2-3, 2006

79) 池袋 一典, 小笠原 大輔 , 金子 清俊, 早出 広司: マウスプリオンアプタマーの探索とそのセンシングへの応用 (Selection of the aptamer for prion and its application to sensor system). 日本化学会バイオテクノロジー部会. 京都, 9.28-30, 2006

80) 山本真央, 高須美和, 徳永勝士, 数藤由美子, 平井百樹, 北條浩彦, 功刀浩, 上野美華子, 南光進一郎: 均衡型染色体転座部位

における双極性障害疾患感受性遺伝子探索. 第28回日本分子生物学会、福岡, 2005

81) 桑田　一夫: 『プリオン病の基本メカニズムの解明と治療薬開発』～21 世紀における新創薬パラダイス～. 社団法人　岐阜県獣医師会. 美濃加茂, 11.12, 2004

82) 桑田　一夫: 感染する異常たんぱく質－プリオン複製の謎－. 独立行政法人　科学技術振興機構. 岐阜県健康科学センター, 11.18, 2004

83) 桑田　一夫: 蛋白質の立体構造とダイナミクスに基づく論理的創薬法及びそれによる抗プリオン薬の開発. 国立感染症研究所学友会シンポジウム. 東京, 2.14, 2005

84) 桑田一夫, 中村寛則, 鎌足雄司, 松本友治: Prion は Downhill Folder か？生物物理日本生物物理学会第 43 回年会: 11 月, 2005

85) 桑田一夫: プリオンの構造ダイナミクスと治療薬開発. プロテイン・クロストークサロン'05. 茨城, 3 月, 2005

86) 桑田一夫: Slow conformational dynamics, Prion protein. 理研シンポジウム Pressure and protein dynamics. 兵庫, 3 月,2005

87) 桑田一夫: プリオンの立体構造解析と抗プリオン薬の in silico デザイン. 医薬基盤研究所シンポジウム「in silico 創薬の現状と展望」. 東京, 11 月, 2005

88) 小見和也, 徳永勝士, 北條浩彦: RNAi による遺伝子発現ノックダウンを用いた神経疾患関連遺伝子の機能解析. 第 27 回日本分子生物学会、神戸, 2004

G. 知的所有権の出願・取得状況（予定を含む。）

1. 特許取得予定

特許出願番号： 2005-116177
発明者：北條浩彦
発明の名称：「対立遺伝子に対する特異的RNAiの評価方法」
出願人：財団法人ヒューマンサイエンス振興財団とプロメガ株式会社との共同出願
出願日：平成17年4月13日

2. 実用新案登録　なし

3. その他　なし

研究成果の刊行に関する一覧表

書籍

著者氏名	論文タイトル名	書籍全体の編集者名	書　籍　名	出版社名	出版地	出版年	ページ
Hachiya NS, Yamada M, Watanabe K, Jozuka A, Ohkubo T, Kozuka Y, Sakasegawa Y, Kaneko K	Targeting of cytosolic PrP^C via a novel 14-3-3-Tom 70-mitochondrial BCL-2 pathway induces mitochondrial apoptosis	Kitamoto T	PRIONS-Food and Drug Safety-	Springer-Verlag	Tokyo	2005	207-208
Hachiya NS, Watanabe K, Sakasegawa Y, Kaneko K	Microtubule-dependent intracellular trafficking of cellular prion protein	Kitamoto T	PRIONS-Food and Drug Safety-	Springer-Verlag	Tokyo	2005	209-210
Sakasegawa Y, Kishida H, Watanabe K, Hachiya NS, Kaneko K	HSP90 modifies the conformation of recombinant mouse prion protein in vitro	Kitamoto T	PRIONS-Food and Drug Safety-	Springer-Verlag	Tokyo	2005	211-212
Hachiya NS, Yamada M, Jozuka A, Kozuka Y, Sakasegawa Y, Kaneko K	Purification and characterization of a novel ATP-dependent robust protein-unfoldase, Unfoldin	Kitamoto T	PRIONS-Food and Drug Safety-	Springer-Verlag	Tokyo	2005	213-214
Iwanami N, Sankawa U, Saido TC, Yamakawa Y, Nishijima M, Kaneko K	Screening study of prion binding agents and their inhibitory effect on the conversion of prion protein	Kitamoto T	PRIONS-Food and Drug Safety-	Springer-Verlag	Tokyo	2005	261-263
Kuwata K	Semi-classical Quantization of Protein Dynamics: Novel NMR Relaxation Formalism and its Application to Prion	Kitamoto K	PRIONS- Food and Drug Safety	Springer Tokyo	Tokyo	2005	155-170
Hachiya NS Kaneko K	Investigation of laser microdissected inclusion bodies	Berns M, Greulich KO	Method in Cell Biology	Academic Press	New York	2007	in press

金子清俊	プリオン病の治療法開発	金澤一郎, 柴崎浩, 東儀英夫	先端医療シリーズ30 神経内科 「神経内科の最新医療」	先端医療技術研究所	東京	2004	255-259
八谷如美, 金子清俊	プリオン病の治療 - 現状と将来展望	柳沢信夫, 篠原幸人, 岩田誠, 清水輝夫, 寺本明	Annual Review2005 神経	中外医学社	東京	2005	90-95
金子清俊	プリオン病.	三木哲郎	日常診療に活かす老年病ガイドブック-認知症・うつ・睡眠障害の診療の実際-	Medical View	東京	2005	173-179
金子清俊	不思議なプリオン病	井原康夫	脳はどこまでわかったか. 朝日選書771	朝日新聞社	東京	2005	771-
金子清俊	牛海綿状脳症と人変異型クロイツフェルト・ヤコブ病	本間清一	食品の安全性評価の考え方 –畜産食品を中心に-	日本栄養・食料学会	東京	2006	29-45
金子清俊	科学者が語るBSEのはなし	金子清俊	科学者が語るBSEのはなし	コープ出版	東京	2006	1-34
桑田一夫	２０世紀の２大発見－量子力学と分子生物学	桑田一夫	『論理的創薬入門－構造生物学に基づくアプローチ』	共立出版	東京	2006.6	9-24
桑田一夫	フーリエ変換とタンパク室・核酸の基本立体構造	桑田一夫	『論理的創薬入門－構造生物学に基づくアプローチ』	共立出版	東京	2006.6	25-49
桑田一夫	タンパク室・核酸の構造ダイナミクス	桑田一夫	『論理的創薬入門－構造生物学に基づくアプローチ』	共立出版	東京	2006.6	91-108
桑田一夫	計算機実験の基礎	桑田一夫	『論理的創薬入門－構造生物学に基づくアプローチ』	共立出版	東京	2006.6	137-145
桑田一夫	分子構造と生理機能	桑田一夫	『論理的創薬入門－構造生物学に基づくアプローチ』	共立出版	東京	2006.6	168-181
桑田一夫	タンパク質の構造異常	桑田一夫	『論理的創薬入門－構造生物学に基づくアプローチ』	共立出版	東京	2006.6	182-194
桑田一夫	タンパク質のコンホメーション制御－分子手術法	桑田一夫	『論理的創薬入門－構造生物学に基づくアプローチ』	共立出版	東京	2006.6	195-209

北條浩彦	巻頭ガイド 第２章 第６章 用語解説	程久美子 北條浩彦	RNAi実験 なるほどQ＆A	羊土社	東京	2006	60-68 115-131

雑誌

発表者氏名	論文タイトル名	発表誌名	巻号	ページ	出版年
Hachiya NS, Watanabe K, Sakasegawa Y, Kaneko K	Microtubules-associated intracellular localization of the NH2-terminal cellular prion protein fragment.	Biochem Biophys Res Commun	313	818-823	2004
Tremblay P, Ball HL, Kaneko K, Groth D, Hegde RS, Cohen FE, DeArmond SJ, Prusiner SB, Safar SJ	Mutant PrP^{Sc} Conformers Induced by a Synthetic Peptide and Several Prion Strains.	J Virol	78	2088–2099	2004
Hachiya NS, Watanabe K, Yamada M, S akasegawa Y, Kaneko K	Anterograde and retrograde intracellular trafficking of fluorescent cellular prion protein.	Biochem Biophys Res Commun	315	802-807	2004
Kishida H, Sakasegawa Y, Watanabe K, YamakawaY, Nishijima M, Kuroiwa Y, Hachiya NS, Kaneko K	Non-glycosylphosphatidylinositol (GPI)-anchored recombinant prion protein with dominant-negative mutation inhibits PrP^{Sc} replication *in vitro*.	Amyloid	11	14-20	2004
Hachiya NS, Sakasegawa Y, Jozuka A, Tsukita S, Kaneko K	Interaction of D-lactate dehydrogenase protein 2 (Dld2p) with F-actin: Implication for an alternative function of Dld2p.	Biochem Biophys Res Commun	319	78-82	2004
Hachiya NS, Sakasegawa Y, Sasaki H, Jozuka A, Tsukita S, Kaneko K	Oligomeric Aip2p/Dld2p forms a novel grapple-like structure and has an ATP-dependent F-actin conformation modifying activity *in vitro*.	Biochem Biophys Res Commun	320: 2004	1271-1276,	2004

Hachiya NS, Sakasegawa Y, Sasaki H, Jozuka A, Tsukita S, Kaneko K	Oligomeric Aip2p/Dld2p modifies the protein conformation of both properly-folded and misfolded substrates *in vitro*.	Biochem Biophys Res Commun	323:	339-344,	2004
Hachiya NS, Yamada M, Watanabe K, Jozuka A, Ohkubo T, Sano K, Takeuchi Y, Kozuka Y, Sakasegawa Y, Kaneko K	Mitochondrial localization of cellular prion protein (PrP^C) invokes neuronal apoptosis in aged transgenic mice overexpressing PrP^C.	Neurosci Lett	374	98-103	2005
Hachiya NS, Watanabe K, Kawabata MY, Jozuka A, Ohkubo T, Kozuka Y, Sakasegawa Y, Kaneko K	A disease isoform of fluorescent prion protein (PrP) with Y145STOP induces mitochondria-mediated apoptosis and forms PrP aggregates.	Biochem Biophys Res Commun	327	894-899	2005
Hachiya NS, Yamada M, Watanabe K, Jozuka A, Ohkubo T, Sano K, Takeuchi Y, Kozuka Y, Sakasegawa Y, Kaneko K	Mitochondrial localizationof cellular prion protein (PrP^C) invokes neuronal apoptosis in aged transgenic mice overexpressing PrP^C	Neurosci Lett	74	98-103	2005
Hachiya NS, Watanabe K, Kawabata MY, Jozuka A, Ohkubo T, Kozuka Y, Sakasegawa Y, Kaneko K	Prion protein with Y145STOP mutation induces mitochondria-mediated apoptosis and PrP-containing deposits in vitro	Biochem Biophys Res Commun	327	894-899	2005

Tamura Y, Sakasegawa Y, Omi K, Kishida H, Asada T, Kimura H, Tokunaga K, Hachiya NS, Kaneko K, Hohjoh H	Association study of the chemokine, CXC motif, ligand 1 (CXCL1) gene with sporadic Alzheimer's disease in a Japanese population	Neurosci Lett	379	149-151	2005
Noma T, Ikebukuro K, Sode K, Ohkubo T, Sakasegawa Y, Hachiya NS, Kaneko K	Screening of DNA aptamers against multiple proteins in tissue	Nucleic Acids Symposium Series	49	357-358	2005
Hachiya NS, Ohkubo T, Kozuka Y, Yamazaki M, Mori O, Mizusawa H, Sakasegawa Y, Kaneko K	More than a 100-fold increase in immunoblot signals of laser-microdissected inclusion bodies with an excessive aggregation property by oligomeric actin interacting protein 2/d-lactate dehydrogenase protein 2	Anal Biochem	347	106-111	2005
Omi K, Hachiya NS, Tokunaga K, Kaneko K	siRNA-mediated inhibition of endogenous Huntington disease gene expression induces an aberrant configuration of the ER network *in vitro*	Biochem Biophys Res Commun	338	1229-1235	2005
Kaneko K, Hachiya NS	Hypothesis: Gut as source of motor neuron toxin in the development of ALS	Med Hypotheses	66	438-439	2006
Ohkubo T, Sakasegawa Y, Toda H, Kishida H, Arima K, Yamada M, Takahashi H, Mizusawa H, Hachiya NS, Kaneko K	Three-repeat tau 69 is a major tau isoform in laser-microdissected Pick bodies	Amyloid	13	1-5	2006
Kaneko K, Hachiya NS	The alternative role of 14-3-3 zeta as a sweeper of misfolded proteins in disease conditions	Med Hypotheses	67	169-171	2006

Furuya K, Kawahara N, Yamakawa Y, Kishida H, Hachiya NS, Nishijima M, Kirino T, Kaneko K	Intracerebroventricular delivery of dominant negative prion protein in a mouse model of iatrogenic Creutzfeldt-Jakob disease after dura graft transplantation	Neurosci Lett	402	222-226	2006
Noma T, Ikebukuro K, Sode K, Ohkubo T, Sakasegawa Y, Hachiya NS, KanekoK	Selection of DNA aptamers toward a specific protein in complex targets	Biotechnol Lett	28	1377-1381	2006
Ohnishi Y, Tokunaga K, Kaneko K, Hohjoh H	Assessment of allele-specific gene silencing by RNA interference with mutant and wild-type reporter alleles	J RNAi Gene silencing	2	154-160	2006
Hachiya NS, Imagawa M, Kaneko K	The possible role of protein X, a putative auxiliary factor in pathological prion replication, in regulating a physiological endoproteolytic cleavage of cellular prion protein	Med Hypotheses		in press	2007
Soeda A, Nakashima T, Okumura A, Kuwata K, Shinoda J, Iwama T.	Cognitive impairment after traumatic brain injury-a functional magnetic resonance imaging study using the Stroop task.	Neuroradiology	47(7)	501-506	2005
Hashimoto K, Kato Z, Nagase T, Shimozawa N, Kuwata K, Omoya K, Li A, Matsukuma E, Yamamoto Y, Ohnishi H, Tochio H, Shirakawa M, Suzuki Y, Wanders RJ, Kondo N.	Molecular Mechanism of a Temperature-Sensitive Phenotype in Peroxisomal Biogenesis Disorder.	Pediatric Research	58(2)	263-269	2005

Kimura K, Moriwaki H, Nagaki M, Saio M, Nakamoto Y, Naito M, Kuwata K, Chisari FV	Pathogenic role of B cells in anti-CD40 caused necroinflammatory liver disease	Am J Pathol	168(3)	786-795	2006
Sukegawa HK, Kato Z, Nakamura H, Tomatsu S, Fukao T, Kuwata K, Orii T, Kondo N	Effect of Hunter disease (mucopolysaccharidosis type II) mutations on molecular phenotypes of iduronate-2-sulfatase : Enzymatic activity, protein processing and structural analysis	J Inherit Metab Dis	29	755-761	2006
Ohnishi Y, Tokunaga K, Hohjoh H	Influence of assembly of siRNA elements into RNA-induced silencing complex (RISC) by fork-siRNA duplex carrying nucleotide mismatches at the 3'- or 5'-end of the sense-stranded siRNA element	Biochem Biophys Res Commun	329	516-521	2005
Tamura Y, Sakasegawa Y, Omi K, Kishida H, Asada T, Kimura H, Tokunaga K, Hachiya NS, Kaneko K, Hohjoh H	Association study of the chemokine, CXC motif, ligand 1 (CXCL1) gene with sporadic Alzheimer's disease in a Japanese population.	Neurosci Lett	379	149-151	2005
Sakai T, Hohjoh H	Gene silencing analyses against amyloid precursor protein (APP) gene family by RNA interference.	Cell Biol Int	30	952-956	2006
Ohashi J, Naka I, Toyoda A, Takasu M, Tokunaga K, Ishida T, Sakaki Y, Hohjoh H	Estimation of the species-specific mutation rates of the DRB1 locus in human and chimpanzee.	Tissue Antigens	68	427-431	2006

Kawashima M, Tamiya G, Oka A, Hohjoh H, Juli T, Ebisawa T, Honda Y, Inoko H, Tokunaga K	Genome-wide association analysis of human narcolepsy and a new resistance gene.	Am J Hum Genet	79	252-263	2006
金子清俊	BSE, SARS, 鳥インフルエンザ等の感染症とつきあう方法	環境会議	21	214-217	2004
八谷如美, 金子清俊	プリオン病治療の新たな可能性	バイオインダストリー	21	60-66	2004
金子清俊	BSE (牛海綿状脳症)とその食へのリスクについて	日本食肉加工情報	647	19-29	2004
八谷如美, 金子清俊	BSEとプリオンの増殖・感染機構	蛋白質・核酸・酵素	49	1005-1007	2004
八谷如美, 金子清俊	プリオン病とミトコンドリアの接点	医学のあゆみ	209	1015-1017	2004
金子清俊	プリオン病	小児内科	36	1166-1169	2004
金子清俊	プロテオミクスによる神経疾患の病態解析	神経研究の進歩	48	700-706	2004
金子清俊	ウシ海綿状脳症（BSE）	現代化学	404	32-36	2004
金子清俊	プルシナー論文を読むコッホの四原則を証明	現代化学	404	39	2004
金子清俊	BSE検査	日本医事新報	4200	88-89	2004
逆瀬川裕二, 八谷如美, 金子清俊	プリオン病	国立医療学誌「医療」	58	658-660	2004
金子清俊	牛海綿状脳症/プリオン病.	日本内科学会誌	93	2363-2368	2004
金子清俊	クロイツフェルト・ヤコブ病.	臨床と微生物	32	69-72	2005
八谷如美, 金子清俊	新しいシャペロンの発見 – 神経難病の治療へ -.	科学	75	283-285	2005
八谷如美, 金子清俊	プリオン研究の進展	VIRUS REPORT	2	14-19	2005
金子清俊	vCJD (変異型クロイツフェルト・ヤコブ病)	日本評論社「からだの科学」	244	95	2005
金子清俊	BSEと食の安全	日本薬剤師会雑誌	57	81-84	2005
金子清俊	科学と行政 – 科学者とBSE対策 -	現代化学	416	60-63	2005

八谷如美, 金子清俊	プリオン病の現状-牛海綿状脳症と変異型CJDを中心に-	LABIO 21	22	5-10	2005
八谷如美, 金子清俊	牛海綿状脳症 (BSE) と変異型CJD	Bios.	10	7-8	2005
金子清俊	特集「プリオン病」	医学のあゆみ	215	875	2005
八谷如美	特集「プリオン病」	医学のあゆみ	215		2005
金子清俊	理系の説明責任. BSE問題をめぐって	科学	76	52-55	2006
八谷如美, 金子清俊	プリオン蛋白質異常化の分子機構	化学療法の領域	22	63-68	2006
金子清俊	牛海綿状脳症と変異型クロイツフェルト・ヤコブ病	TMDC MATE	242	12-13	2006
金子清俊	プリオン病 - 牛海綿状脳症 (BSE)と変異型クロイツフェルト・ヤコブ病	BRAIN	83	4-5	2006
八谷如美, 金子清俊	正常型プリオンたんぱく質の正体は？ - その推定される機能 -	現代化学	422	26-31	2006
金子清俊	食について考える - 「安全」と「安心」とは -	建設労働の広場	59	52-56	2006
金子清俊	米国産牛肉輸入再開をめぐる問題について	肉牛ジャーナル	11	56-57	2006
金子清俊, 神田敏子, 水澤英洋, 山内一也	BSEの危険度はどこまでわかったのか -何が問われるべきか-	科学	76	1105-1112	2006
八谷如美, 金子清俊	プリオンたんぱく質は正常人では何をしているのか？	科学	76	1138-1142	2006
八谷如美, 金子清俊	正常Prion蛋白の機能と異常化 (感染)のメカニズム	Brain Medical		印刷中	2007
八谷如美, 金子清俊	正常Prion蛋白とその機能	日本臨床		印刷中	2007
桑田一夫	バイオインフォーマティクスによるプリオン病治療薬の開発	化学療法の領域	22	87-93	2006
桑田一夫	連載“話題のウイルス”NO.12 プリオン	Drug Delivery System (DDS)	21	156-157	2006
山口圭一, 松本友治, 児玉耕太, 岸直人, 桑田一夫	プリオン病の発症と伝播機構－特集 アミロイドの謎は解けるか？：プリオン病・アルツハイマー病・透析アミロイドーシスなどの病態を紐解く－	細胞工学	26 (2)	151-155	2007

後藤祐児, 桑田一夫, 関島良樹, 田中元雅, 内木宏延, 永井義隆, 松崎勝巳, 樋口京一	アミロイドーシス発症の分子機構解明を目指して：現状と展望，夢ー特集 アミロイドの謎は解けるか？：プリオン病・アルツハイマー病・透析アミロイドーシスなどの病態を紐解くー	細胞工学	26（2）	181-185	2007
北條　浩彦	神経・筋疾患治療へのRNAi応用	神経治療学	23	31-36	2006
北條　浩彦	RNAi効果の評価法	バイオテクノロジージャーナル	6	51-57	2006

Available online at www.sciencedirect.com
SCIENCE DIRECT®
Biochemical and Biophysical Research Communications 315 (2004) 802–807
BBRC
www.elsevier.com/locate/ybbrc

Anterograde and retrograde intracellular trafficking of fluorescent cellular prion protein

Naomi S. Hachiya, Kota Watanabe, Makiko Yamada, Yuji Sakasegawa, and Kiyotoshi Kaneko*

Department of Cortical Function Disorders, National Institute of Neuroscience (NIN), National Center of Neurology and Psychiatry (NCNP), and Core Research for Evolutional Science and Technology (CREST), Japan Science and Technology Agency, Tokyo 187-8502, Japan

Received 22 January 2004

Abstract

In order to investigate the microtubule-associated intracellular trafficking of the NH2-terminal cellular prion protein (PrP^C) fragment [Biochem. Biophys. Res. Commun. 313 (2004) 818], we performed a real-time imaging of fluorescent PrP^C (GFP-PrP^C) in living cells. Such GFP-PrP^C exhibited an anterograde movement towards the direction of plasma membranes at a speed of 140–180 nm/s, and a retrograde movement inwardly at a speed of 1.0–1.2 μm/s. The anterograde and retrograde movements of GFP-PrP^C were blocked by a kinesin family inhibitor (AMP-PNP) and a dynein family inhibitor (vanadate), respectively. Furthermore, anti-kinesin antibody (α-kinesin) blocked its anterograde motility, whereas anti-dynein antibody (α-dynein) blocked its retrograde motility. These data suggested the kinesin family-driven anterograde and the dynein-driven retrograde movements of GFP-PrP^C. Mapping of the interacting domains of PrP^C identified amino acid residues indispensable for interactions with kinesin family: NH2-terminal mouse (Mo) residues 53–91 and dynein: NH2-terminal Mo residues 23–33, respectively. Our findings argue that the discrete N-terminal amino acid residues are indispensable for the anterograde and retrograde intracellular movements of PrP^C.

Keywords: Cellular prion protein; Green fluorescent protein; Microtubules; Kinesin family; Dynein

The posttranslational conformational change of the cellular isoform of prion protein (PrP^C) into the scrapie isoform of prion protein (PrP^{Sc}) is the fundamental process underlying the pathogenesis of the prion disease [2,3]. An initial degradation of PrP^C involves cleavage of the NH2-terminal fragment to produce a COOH-terminal 17-kDa polypeptide which was found in a Triton X-100 insoluble fraction [4], of which the cleavage site was mapped at the amino acid residues between the 3F4 (amino acids 108/111 in mouse (Mo) PrP) and the 13A5 (amino acids 138 in Mo PrP) epitopes [4–6]. Several groups reported that NH2-terminal fragment of the PrP functions as a putative targeting element [7,8] and is essential for both transport to the plasma membrane and modulation of endocytosis [9]. GFP-tagged version of PrP^C was found to be properly anchored at the cell surface and its distribution pattern was similar to that of the endogenous PrP^C, with labelling at the plasma membrane and in an intracellular perinuclear compartment [10–14].

We previously demonstrated the microtubule-associated intracellular localization of the NH2-terminal fluorescent PrP^C fragment [1] in Mo neuroblastoma neuro2a (N2a), known to be infectable with PrP^{Sc} [15] and HpL3-4 cells, a hippocampal cell line established from *prnp* gene-ablated mice [16], by utilizing double-labelled PrP^C. At a steady state level, we detected NH_2-terminally fluorescent-tagged PrP^C predominantly in the intracellular compartments, COOH-terminally fluorescent-tagged PrP^C mostly at the cell surface membranes overlapping with lipid rafts, and PrP^C in full length with the merged color in Golgi compartments. The NH_2-terminal PrP^C fragment, which may not reflect the distribution to any single specific organelle, congregated in the cytosol after the treatment with a microtubule

* Corresponding author. Fax: +81-42-346-1748.
E-mail address: kaneko@ncnp.go.jp (K. Kaneko).

0006-291X/$ - see front matter © 2004 Elsevier Inc. All rights reserved.
doi:10.1016/j.bbrc.2004.01.126

depolymerizer (nocodazole). Such microtubule-associated intracellular localization required at least the 1–91 amino acid residues of the NH2-terminal PrP^C fragment.

With this background, we performed a follow-up study of intracellular GFP-PrP^C by a real-time imaging, which demonstrated the anterograde and retrograde intracellular movements of the NH_2-terminal PrP^C fragment in N2a and HpL3-4 cells.

Materials and methods

Construction of GFP-PrP and the deletion mutants. GFP-PrP constructs were made as previously described [1], and the resulted plasmid was designated pSPOX-MHM2PrP::GFP. The series of deletion mutants were amplified by PCR from the pSPOX-MHM2PrP::GFP [1] using 5′-GCA ACC GTT ACC CAC CTC AGG GGG GTA CCC ATA ATC AGT GGA ACA AGC CC-3′ as the forward primer and the following backward primers: 5′-CTG AGG TGG GTA ACG GTT GCC TCC AGG GCT-3′ (for amino acid residues Δ53–91 in Mo PrP), 5′-CTG ATG TCG GCC TCT GCA AAG GTA TGG TGA GC-3′ and 5′-TTT GCA GAG GCC GAC ATC AGT CCA CAT AGT-3′ (Δ23–33), digested with *Bam*HI and *Xho*I, and replaced with the *Bam*HI–*Xho*I fragment of pSPOX-MHM2PrP::GFP [17]. The resulted plasmids were verified by direct DNA sequencing.

Antibodies and drugs. Anti-kinesin and anti-dynein antibodies were purchased from Santa Cruz Biotechnology, and anti-γ-tubulin antibody was purchased from Sigma. Vanadate and AMP-PNP were purchased from CHEMICON and Sigma, respectively. Nocodazole was purchased from Sigma.

Cell cultures, DNA transfection, and drug treatments. Mo neuroblastoma neuro2a (N2a) cells known to be infectable with PrP^{Sc} [15] were obtained from American Tissue Culture Collection. A hippocampal cell line established from *prnp* gene-ablated mice (HpL3-4) was kindly provided by Dr. T. Onodera. Cells were grown and maintained at 37 °C in MEM supplemented with 10% fetal bovine serum. N2a and HpL3-4 cells were transiently transfected with each construct using a DNA transfection kit (Lipofectamin, Gibco-BRL). Western blot analyses were performed as described [17]. Vanadate (10 μM at 30 °C for 30 min) and AMP-PNP (100 μM and 2 mM at 30 °C for 30 min) treatments were performed according to the previous report [18].

Immunofluorescent microscopy. For indirect immunofluorescence analysis, fluorescent PrP^C-transfected N2a cells were rinsed with PBS with Ca^{2+} and Mg^{2+} (PBS(+)) and then fixed with 10% formalin in 70% PBS(+) for 30 min at room temperature. After four washes with PBS(−), the fixed cells were incubated 10% FBS in PBS(−) for 30 min at room temperature. They were then incubated for 1 h at room temperature with antibodies at desired concentrations. After four washes with PBS(−), the cells were incubated with either Alexa488 (green) Fluor-conjugated anti-rabbit IgG (Molecular Probes) or Alexa594 (red) Fluor-conjugated anti-mouse IgG (Molecular Probes), diluted 1:200 in PBS, for 1 h at room temperature. The stained cells were washed four times with PBS(−) and mounted with SLOW FADE (Molecular Probes). Samples were imaged with Delta-Vision microscopy system (Applied Precision), out of focus light of the visualized images was removed by interactive deconvolution.

Real-time imaging. To observe living cells, cells were cultured on glass-bottomed dishes (Matsunami) in culture medium without phenol red at 30 °C. Images of cells were collected with a Delta Vision Microscopy System (Applied Precision) equipped with an Olympus IX70 through a cooled CCD camera (Quantix-LC, Photometrics). Fluorescence signals were visualized using a quad beam splitter (Chroma) and the following excitation and emission filter 525/50 nm (Chroma).

In vitro motility assay. For cytosol preparations, N2a cells were collected from 9 cm × 10 dishes, washed and suspended in four volumes of PBS, homogenized, and ultracentrifuged. After ultracentrifugation at 100,000*g* for 60 min, supernatants were collected and used for these experiments. Alexa 594-labelled tubulin (Molecular Probe) was polymerized in PEM buffer (35 mM Pipes, pH 7.0, 0.5 mM EGTA, and 0.5 mM $MgCl_2$). Polymerized tubulin, recombinant GFP-PrP, and cytosol (1 mg/ml) were mixed and incubated at 30 °C for 5 min in PEM buffer in the presence of 1 mM ATP. After incubation, samples were spread onto glass-bottom dishes and then observed with the Delta Vision Microscopy System (Applied Precision).

Results

The intracellular trafficking of fluorescent PrP^C was investigated through the real-time imaging in living cells

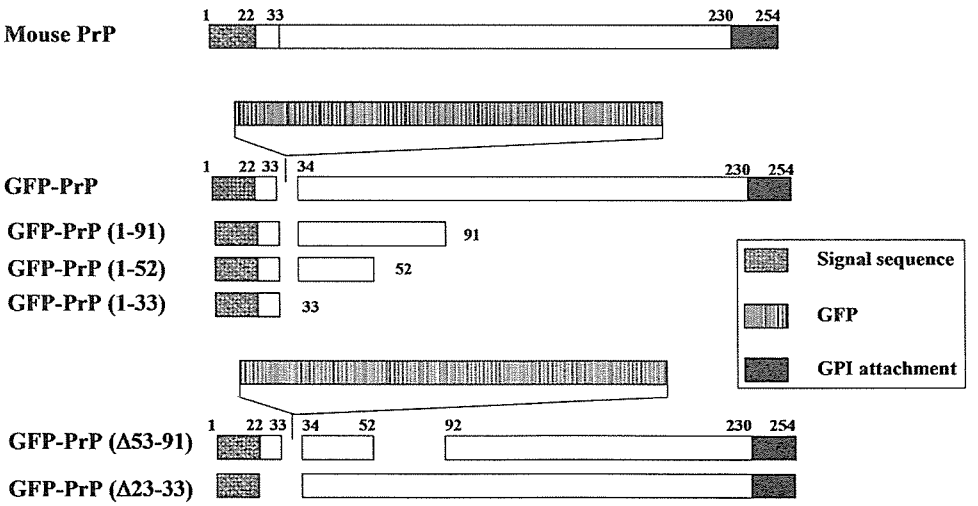

Fig. 1. Immunofluorescent analysis of GFP-PrP^C. The chimeric GFP-PrP constructs including the deletion mutant series used in this study. GFP-PrP (1–91), (1–52), and (1–33) constructs were made as previously described [1]. These recombinant GFP-PrPs were transfected in N2a cells.

by utilizing GFP-PrP constructs (Fig. 1). As results, we revealed that GFP-PrP^C transfected in N2a cells exhibited an anterograde movement towards the direction of plasma membranes at a speed of 140–180 nm/s as well as a retrograde movement inwardly at a speed of 1.0–1.2 μm/s (Fig. 2A). The same results were obtained from other experiments with GFP-PrP^C transfected in HpL3-4 cells (data not shown).

A kinesin family inhibitor of AMP-PNP at a concentration of 100 μM inhibited the anterograde movement of GFP-PrP^C which congregated at an intracellular perinuclear compartment (Fig. 2B), whereas a dynein family inhibitor of vanadate at a concentration of 10 μM inhibited the retrograde movement of GFP-PrP^C which was subsequently detected at the plasma membrane (Fig. 2B) [18]. At a concentration of 2 mM, AMP-PNP inhibited both kinesin and dynein families, and the intracellular motility of GFP-PrP^C was completely blocked (Fig. 2B). The intracellular trafficking of the NH_2-terminal PrP^C fragment was also blocked by the treatment with a microtubule depolymerizer (nocodazole) (data not shown). Furthermore, anti-kinesin antibody (α-kinesin) blocked the anterograde motility of GFP-PrP^C to congregate in an intracellular perinuclear compartment, and anti-dynein antibody (α-dynein) blocked its retrograde motility to reside at a plasma membrane (Fig. 2C).

Next, the deletion mutants (Fig. 1) were used to identify the amino acid residues responsible for the anterograde and retrograde movements of GFP-PrP^C. Truncated constructs with the amino acid residues 1–121, 1–111, and 1–91 in Mo PrP transfected in N2a cells

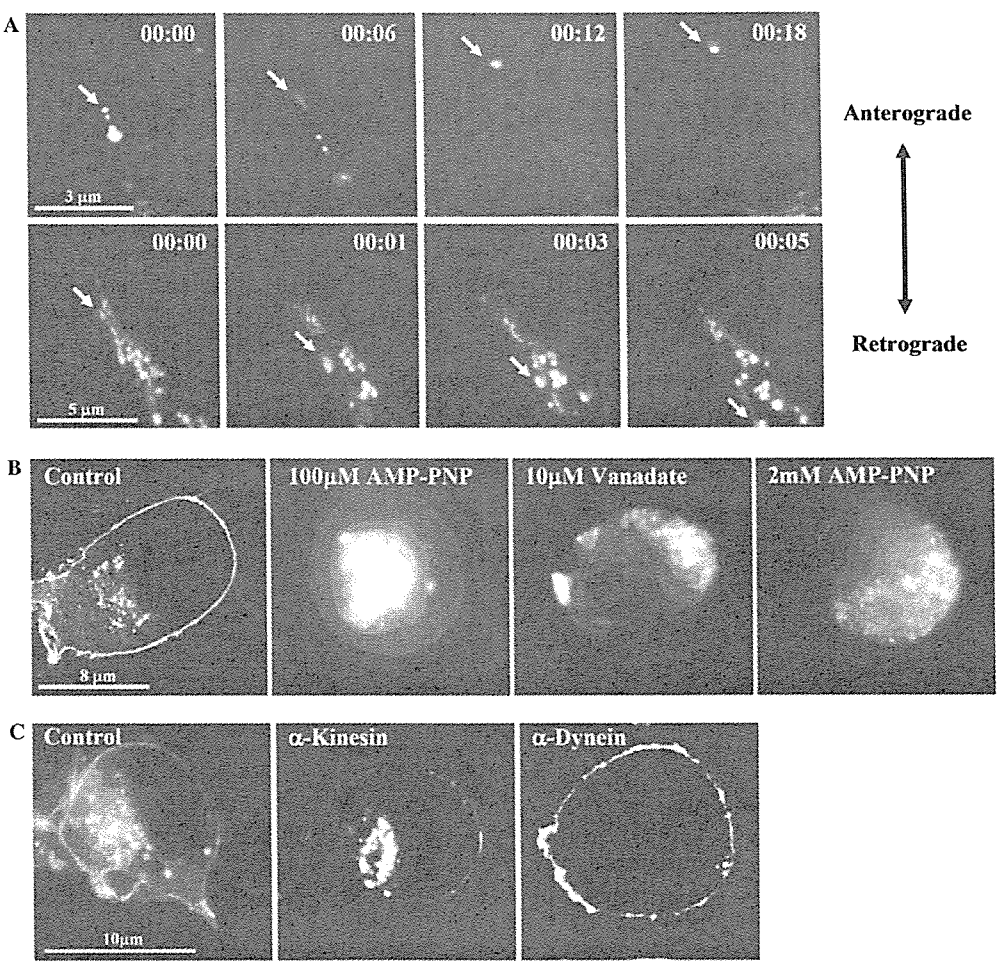

Fig. 2. Intracellular trafficking of GFP-PrP^C by a real-time imaging in living cells, and the drug- or antibody-mediated inhibitions of intracellular movements. (A) Recombinant GFP-PrP^C transfected in N2a cells exhibits an anterograde movement at a speed of 140–180 nm/s (upper panels) and an inward retrograde movement at a speed of 1.0–1.2 μm/s (lower panels). Scale bar (upper panel) = 3 μm and scale bar (lower panel) = 5 μm. (B) A kinesin family inhibitor of AMP-PNP at a concentration of 100 μM inhibited the anterograde movement of GFP-PrP^C which congregates in an intracellular perinuclear compartment. A dynein family inhibitor of vanadate at a concentration of 10 μM inhibits the retrograde movement of GFP-PrP^C which congregates at a plasma membrane. At a concentration of 2 mM, AMP-PNP inhibits both kinesin and dynein families, and the intracellular motility of GFP-PrP^C is completely blocked. Scale bar = 8 μm. (C) Anti-kinesin antibody (α-kinesin) blocks the anterograde motility of GFP-PrP^C and anti-dynein antibody (α-dynein) blocks its retrograde motility.

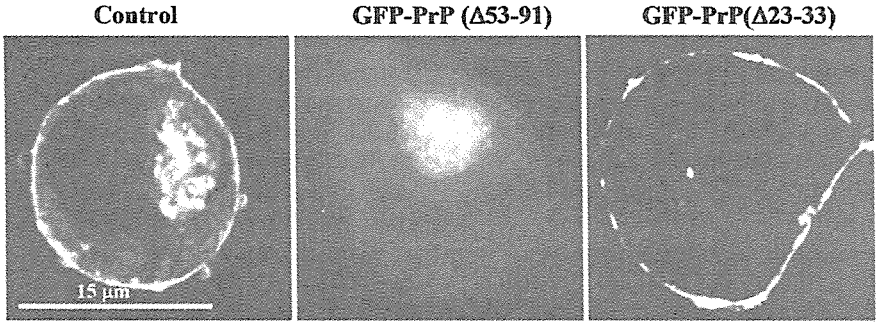

Fig. 3. The amino acid residues responsible for the anterograde and retrograde movements of GFP-PrP^C. The truncated construct of GFP-PrP lacking the amino acid residues 53–91 in Mo PrP loses its anterograde motility and congregates in the intracellular perinuclear compartment. The GFP-PrP construct lacking the amino acid residues 23–33 in Mo PrP loses its retrograde motility and resides at the plasma membrane. Scale bar = 15 μm.

exhibited its proper anterograde and retrograde motilities (data not shown), whereas those with amino acid residues 1–52 and 1–33 in Mo PrP did not [1]. These truncated GFP-PrP^C (1–33 and 1–52) surrounded the γ-tubulin-positive centrosome (microtubule organizing center) (data not shown), suggesting that the truncated GFP-PrP^C with at most 1–52 lost its anterograde movement but those with at least 1–33 still exhibited the dynein-driven retrograde movement. Thus, discrete amino acid residues 53–91 and 23–33 (the first NH2-terminal 1–22 amino acid residues act as a signal sequence) seem to be indispensable for the anterograde and retrograde movements, respectively. In accordance with these observations, the deletion constructs lacking the amino acid residues 53–91 in Mo PrP (GFP-PrP^C (Δ53–91)) lost its anterograde motility and congregated in an intracellular perinuclear compartment, whereas those lacking the amino acid residues 23–33 (GFP-PrP^C (Δ23–33)) lost its retrograde motility and resided at a plasma membrane (Fig. 3).

Finally, an in vitro motility assay [19] was further performed to obtain direct evidence on the interaction at the cytosolic interface between recombinant GFP-PrP and Alexa 594-labelled microtubules with or without cytosolic fractions including kinesin family and dynein motor proteins. However, no movement of GFP-PrP along Alexa 594-labelled microtubules was observed even after the addition of cytosolic fractions (Fig. 4).

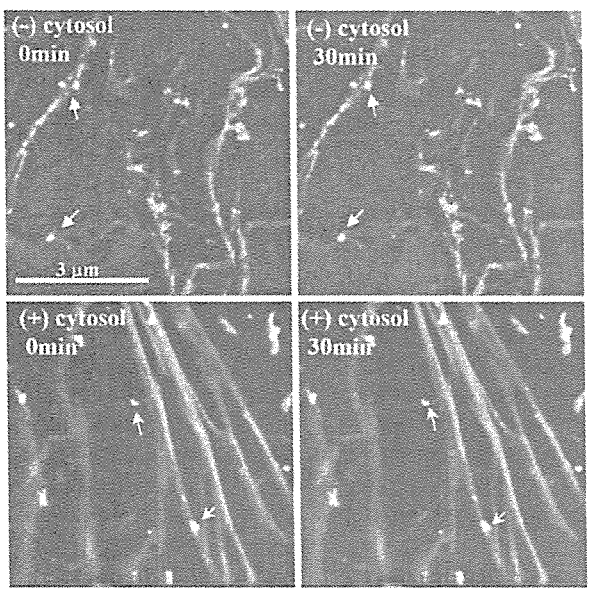

Fig. 4. In vitro motility assay of recombinant GFP-PrP. Polymerized Alexa 594-labelled tubulin, recombinant GFP-PrP, and cytosol (1 mg/ml) were incubated at 30 °C for 5 min in the presence of 1 mM ATP. No movement of recombinant GFP-PrP (arrow heads) along Alexa 594-labelled microtubules was observed for 0–30 min even after the addition of cytosolic fractions (cytosol). Scale bar = 3 μm.

Discussion

We previously reported the microtubule-associated intracellular localization of NH2-terminal PrP^C fragment at a steady state level [1]. A real-time imaging of GFP-PrP^C in living cells, however, has been awaited for further understanding its dynamics along the microtubular network.

Microtubules are essential and ubiquitous cytoskeletal elements composed of heterodimers of α- and β-tubulin, and serve many vital roles, participating in organization of the cytoplasm, in cell motility, and in mitosis [20,21]. In addition to tubulin itself, several microtubule-associated proteins (MAPs) comprise cellular microtubules. The molecular motors that move along microtubules have two origins. The kinesin and myosin families of ATPase motors share a common core structure and may have the same common ancestor as the GTPases involved in signalling and protein synthesis [20,22]. Dynein is part of the family of AAA ATPases [23] that also contribute to protein folding (Hsp100 chaperones), membrane traffic (*N*-ethylmaleimide-sensitive factor or NSF), and DNA synthesis (clamp loader proteins).

Here we showed the anterograde transport of GFP-PrP^C at a speed of 140–180 nm/s and the retrograde transport at a speed of 1.0–1.2 μm/s. These anterograde and retrograde transports of GFP-PrP^C were completely inhibited by AMP-PNP/vanadate which stop the kinesin family/dynein family-driven movements, respectively. Furthermore, anti-kinesin antibody (α-kinesin) blocked the anterograde motility of GFP-PrP^C, and anti-dynein antibody (α-dynein) blocked its retrograde motility. Among the kinesin superfamily, KIF4 moves latex beads from the minus to the plus ends of microtubules, a direction that corresponds to anterograde transport in the axon at a speed of <200 nm/s [24], and dynein is the force-generating protein that produces force in the direction corresponding to retrograde organelle transport at a speed of about 1.4 μm/s in the cell [25–28]. Thus, the anterograde transport of intracellular GFP-PrP^C might be compatible with the speed of the KIF4-driven movement, while the retrograde movement is compatible with that of the dynein-driven movement.

Mapping of the distinct kinesin family-interacting domain and the dynein-interacting domain identified the minimum required amino acid residues in the NH2-terminal PrP^C fragment. The kinesin family-interacting domain (Mo 53–91) is overlapped with an octapeptide repeat region, which is related to the copper metabolism [29–33]. In terms of the PrP^{Sc} formation, the C-terminal domain of PrP^C is known to be insufficient to impede the conversion of the full-length PrP^C molecule to PrP^{Sc} and N-terminally truncated molecules (with residues 23–88 and 23–120 deleted) have reduced dominant-negative activity, and the extreme N-terminal sequence (23KKRPKP29) enhances the dominant-negative phenotype on the formation of PrP^{Sc} [34,35]. This basic sequence is highly conserved in all species studied to date [36]. On the other hand, deletion of the octarepeat sequences (residues 52–91) did not alter PrP^{Sc} formation and dominant-negative inhibition on the formation of PrP^{Sc} [35]. The relevance of these observations to the intracellular trafficking of PrP^C needs to be further investigated.

After internalized, the NH2-terminal PrP^C fragment seems to reside inside vesicles where integral membrane proteins and linker proteins in some cases would be required for the interaction with microtubules to bridge the luminal and cytoplasmic phases across the membranes [1]. Thus, it seems less likely that PrP^C is engaged in the direct interaction with the motor molecules, which is compatible with the fact that the in vitro motility assay failed to show that recombinant GFP-PrP directly moved along Alexa 594-labelled microtubules.

It is also important to identify how many NH2-terminal PrP^C fragments reside in each PrP^C-positive vesicle. In order to answer this question, a single fluorescent molecule is a good potential source because it can emit only one photon at a time. Otherwise it is indispensable to utilize a technique which allows us to know how many photons emit from each PrP^C molecule. Unfortunately, we are currently unable to utilize these techniques. Nonetheless, our results shed a new right on the mechanisms underlying the intracellular trafficking of PrP^C.

Acknowledgments

We greatly thank T. Onodera for providing us the HpL3-4 cell line, E. Nannri, K. Ishibashi, C. Ota, and Y. Yamaura for technical assistance. This work was supported by grants from the Core Research for Evolutional Science and Technology (CREST) of Japan Science and Technology Corporation, Health and Labour Sciences Research Grants, Research on Advanced Medical Technology, nano-001, and the Ministry of Health, Labor and Welfare of Japan.

References

[1] N. Hachiya, K. Watanabe, Y. Sakasegawa, K. Kaneko, Microtubules-associated intracellular localization of the NH2-terminal cellular prion protein fragment, Biochem. Biophys. Res. Commun. 313 (2004) 818–823.
[2] S.B. Prusiner, D.C. Bolton, D.F. Groth, K.A. Bowman, S.P. Cochran, M.P. McKinley, Further purification and characterization of scrapie prions, Biochemistry 21 (1982) 6942–6950.
[3] S.B. Prusiner, P. Peters, K. Kaneko, A. Taraboulos, V. Lingappa, F.E. Cohen, S.J. DeArmond, Cell Biology of Prions, Cold Spring Harbor, New York, 1999.
[4] A. Taraboulos, M. Scott, A. Semenov, D. Avrahami, L. Laszlo, S.B. Prusiner, Cholesterol depletion and modification of COOH-terminal targeting sequence of the prion protein inhibit formation of the scrapie isoform, J. Cell Biol. 129 (1995) 121–132.
[5] M. Rogers, D. Serban, T. Gyuris, M. Scott, T. Torchia, S.B. Prusiner, Epitope mapping of the Syrian hamster prion protein utilizing chimeric and mutant genes in a vaccinia virus expression system, J. Immunol. 147 (1991) 3568–3574.
[6] K.-M. Pan, N. Stahl, S.B. Prusiner, Purification and properties of the cellular prion protein from Syrian hamster brain, Protein Sci. 1 (1992) 1343–1352.
[7] S.-L. Shyng, J.E. Heuser, D.A. Harris, A glycolipid-anchored prion protein is endocytosed via clathrin-coated pits, J. Cell Biol. 125 (1994) 1239–1250.
[8] S.-L. Shyng, K.L. Moulder, A. Lesko, D.A. Harris, The N-terminal domain of a glycolipid-anchored prion protein is essential for its endocytosis via clathrin-coated pits, J. Biol. Chem. 270 (1995) 14793–14800.
[9] M. Nunziante, S. Gilch, H.M. Schatzl, Essential role of the prion protein N terminus in subcellular trafficking and half-life of cellular prion protein, J. Biol. Chem. 278 (2003) 3726–3734.
[10] K.S. Lee, A.C. Magalhaes, S.M. Zanata, R.R. Brentani, V.R. Martins, M.A. Prado, Internalization of mammalian fluorescent cellular prion protein and N-terminal deletion mutants in living cells, J. Neurochem. 79 (2001) 79–87.
[11] A.C. Magalhaes, J.A. Silva, K.S. Lee, V.R. Martins, V.F. Prado, S.S.G. Ferguson, M.V. Gomez, R.R. Brentani, M.A.M. Prado, Endocytic intermediates involved with the intracellular trafficking of a fluorescent cellular prion protein, J. Biol. Chem. 277 (2002) 33311–33318.
[12] A. Negro, C. Ballarin, A. Bertoli, M.L. Massimino, M.C. Sorgato, The metabolism and imaging in live cells of the bovine prion

protein in its native form or carrying single amino acid substitutions, Mol. Cell. Neurosci. 17 (2001) 521–538.
[13] H. Lorenz, O. Windl, H.A. Kretzschmar, Cellular phenotyping of secretory and nuclear prion proteins associated with inherited prion diseases, J. Biol. Chem. 277 (2002) 8508–8516.
[14] L. Ivanova, S. Barmada, T. Kummer, D.A. Harris, Mutant prion proteins are partially retained in the endoplasmic reticulum, J. Biol. Chem. 276 (2001) 42409–42421.
[15] D.A. Butler, M.A. Scott, J.M. Bockman, D.R. Borchelt, A. Taraboulos, K.K. Hsiao, D.T. Kingsbury, S.B. Prusiner, Scrapie-infected murine neuroblastoma cells produce protease-resistant prion proteins, J. Virol. 62 (1988) 1558–1564.
[16] C. Kuwahara, A.M. Takeuchi, T. Nishimura, K. Haraguchi, A. Kubosaki, Y. Matsumoto, K. Saeki, T. Yokoyama, S. Itohara, T. Onodera, Prions prevent neuronal cell-line death, Nature 400 (1999) 225–226.
[17] M.R. Scott, R. Kohler, D. Foster, S.B. Prusiner, Chimeric prion protein expression in cultured cells and transgenic mice, Protein Sci. 1 (1992) 986–997.
[18] T.A. Schroer, M.P. Sheetz, Role of kinesin and kinesin-associated proteins in organelle transport, in: F.D. Warner, J.R. McIntosh (Eds.), Cell Movement, Alan R. Liss, New York, 1989, pp. 295–306.
[19] A. Kubo, H. Sasaki, A. Yuba-Kubo, S. Tsukita, N. Shiina, Centriolar satellites: molecular characterization, ATP-dependent movement toward centrioles and possible involvement in ciliogenesis, J. Cell Biol. 147 (1999) 969–980.
[20] T.D. Pollard, The cytoskeleton, cellular motility and the reductionist agenda, Nature 422 (2003) 741–745.
[21] J. Howard, A.A. Hyman, Dynamics and mechanics of the microtubule plus end, Nature 422 (2003) 753–758.
[22] R.D. Vale, R.A. Milligan, The way things move: looking under the hood of molecular motor proteins, Science 288 (2000) 88–95.
[23] G. Mocz, I.R. Gibbons, Model for the motor component of dynein heavy chain based on homology to the AAA family of oligomeric ATPases, Structure (Camb) 9 (2001) 93–103.
[24] N. Hirokawa, Kinesin and dynein superfamily proteins and the mechanism of organelle transport, Science 279 (1998) 519–526.
[25] R.D. Vale, B.J. Schnapp, T. Mitchison, E. Steuer, T.S. Reese, M.P. Sheetz, Different axoplasmic proteins generate movement in opposite directions along microtubules in vitro, Cell 43 (1985) 623–632.
[26] R.D. Vale, T.S. Reese, M.P. Sheetz, Identification of a novel force-generating protein, kinesin, involved in microtubule-based motility, Cell 42 (1985) 39–50.
[27] B.M. Paschal, R.B. Vallee, Retrograde transport by the microtubule-associated protein MAP 1C, Nature 330 (1987) 181–183.
[28] R.B. Vallee, J.S. Wall, B.M. Paschal, H.S. Shpetner, Microtubule-associated protein 1C from brain is a two-headed cytosolic dynein, Nature 332 (1988) 561–563.
[29] D.R. Brown, K. Qin, J.W. Herms, A. Madlung, J. Manson, R. Strome, P.E. Fraser, T. Kruck, A. von Bohlen, W. Schulz-Schaeffer, A. Giese, D. Westaway, H. Kretzschmar, The cellular prion protein binds copper in vivo, Nature 390 (1997) 684–687.
[30] P.C. Pauly, D.A. Harris, Copper stimulates endocytosis of the prion protein, J. Biol. Chem. 273 (1998) 33107–33110.
[31] M.L. Kramer, H.D. Kratzin, B. Schmidt, A. Romer, O. Windl, S. Liemann, S. Hornemann, H. Kretzschmar, Prion protein binds copper within the physiological concentration range, J. Biol. Chem. 276 (2001) 16711–16719.
[32] W.S. Perera, N.M. Hooper, Ablation of the metal ion-induced endocytosis of the prion protein by disease-associated mutation of the octarepeat region, Curr. Biol. 11 (2001) 519–523.
[33] A.P. Garnett, J.H. Viles, Copper binding to the octarepeats of the prion protein. Affinity, specificity, folding, and cooperativity: insights from circular dichroism, J. Biol. Chem. 278 (2003) 6795–6802.
[34] K. Kaneko, L. Zulianello, M. Scott, C.M. Cooper, A.C. Wallace, T.L. James, F.E. Cohen, S.B. Prusiner, Evidence for protein X binding to a discontinuous epitope on the cellular prion protein during scrapie prion propagation, Proc. Natl. Acad. Sci. USA 94 (1997) 10069–10074.
[35] L. Zulianello, K. Kaneko, M. Scott, S. Erpel, D. Han, F.E. Cohen, S.B. Prusiner, Dominant-negative inhibition of prion formation diminished by deletion mutagenesis of the prion protein [In Process Citation], J. Virol. 74 (2000) 4351–4360.
[36] P. Bamborough, H. Wille, G.C. Telling, F. Yehiely, S.B. Prusiner, F.E. Cohen, Prion protein structure and scrapie replication: theoretical, spectroscopic, and genetic investigations, Cold Spring Harb. Symp. Quant. Biol. 61 (1996) 495–509.

Available online at www.sciencedirect.com
SCIENCE DIRECT®
Biochemical and Biophysical Research Communications 319 (2004) 78–82
BBRC
www.elsevier.com/locate/ybbrc

Interaction of D-lactate dehydrogenase protein 2 (Dld2p) with F-actin: implication for an alternative function of Dld2p

Naomi S. Hachiya,[a,b,c] Yuji Sakasegawa,[a,c] Akiko Jozuka,[a,b] Shoichiro Tsukita,[c,d,e] and Kiyotoshi Kaneko[a,b,*]

[a] *Department of Cortical Function Disorders, National Institute of Neuroscience (NIN), National Center of Neurology and Psychiatry (NCNP), Tokyo 187-8502, Japan*
[b] *Core Research for Evolutional Science and Technology (CREST), Japan Science and Technology Agency, Saitama 332-0012, Japan*
[c] *Tsukita Cell Axis Project, Exploratory Research for Advanced Technology (ERATO), Japan Science and Technology Corporation, Saitama 332-0012, Japan*
[d] *Department of Cell Biology, Faculty of Medicine, Kyoto University, Kyoto 606-8501, Japan*
[e] *Solution Oriented Research for Science and Technology (SORST), Japan Science and Technology Corporation, Saitama 332-0012, Japan*

Received 5 April 2004
Available online 12 May 2004

Abstract

D-Lactate dehydrogenase protein 2 [Yeast 15 (1999) 1377; Biochem. Biophys. Res. Commun. 295 (2002) 910] was initially identified as the actin interacting protein 2 (Aip2p) using a two-hybrid screen to search for proteins that interact with actin [Nat. Struct. Biol. 2 (1995) 28], but no other evidence indicating an interaction between Aip2p and actin cytoskeleton has been reported so far. During our search for the protein conformation modifying activity, we serendipitously identified Aip2p isolated from *Saccharomyces cerevisiae* as exhibiting an interaction with F-actin both in vitro and in vivo. Incubation with Aip2p facilitated the formation of the circular form of F-actin in vitro, which exhibited an aberrant trypsin susceptibility. Overexpression of Aip2p induced multi-buds in yeast cells, whereas reduced expression interfered with the formation of the cleavage furrow for the cell division, which was rescued by the introduction of wild-type Aip2p. While Aip2p-treated F-actin in the circular form was negligibly stained by rhodamine-labeled phalloidin (rhodamine–phalloidin) in vitro, rhodamine–phalloidin staining profiles in actin interacting protein 2 gene (AIP2)-modified cells suggested a correlation between the conformation of F-actin and the expression of Aip2p in vivo. AIP2-deleted cells became sensitive to osmotic conditions, a hallmark of actin dysfunction. Finally, immunoprecipitation of yeast cells using anti-Aip2p antibody demonstrated that Aip2p associates with actin. These properties suggest that Aip2p may interact with F-actin in vivo and play an important role in the yeast cell morphology.

Keywords: D-Lactate dehydrogenase protein 2; Actin interacting protein 2; Actin interacting protein 2 gene; F-actin; Trypsin susceptibility assay; Rhodamine–phalloidin staining; Yeast cell morphology

The actin cytoskeleton plays diverse roles in the cell, mediating endocytosis, exocytosis, cell motility, cell polarity, and cytokinesis, each in a spatially localized and temporally controlled manner [4]. Each of these events requires regulation of specific dynamic properties and spatial organization of actin filaments by members of a large collection of actin-binding proteins.

Actin interacting protein 1 (Aip1p) was originally identified using a two-hybrid screen, which has a distinct interaction footprint on actin subdomains III and IV, and is required for normal localization of cofilin to cortical actin patches as well as stimulation of cofilin activity [5]. Aip1p has also been proposed to control actin depolymerization in vivo, and plays an important regulatory role in the rapid remodeling of the cortical actin meshwork [6]. The crystal structure of Aip1p from *Saccharomyces cerevisiae* (*S. cerevisiae*) reveals that overall folding is mediated by two connected

* Corresponding author. Fax: +81-42-346-1748.
E-mail address: kaneko@ncnp.go.jp (K. Kaneko).

0006-291X/$ - see front matter © 2004 Elsevier Inc. All rights reserved.
doi:10.1016/j.bbrc.2004.04.146

seven-bladed propellers [7]. The gene (YDL178w) encoding actin interacting protein 2 (Aip2p) was also identified using a two-hybrid screen to search for *S. cerevisiae* proteins that interact with actin [3], but there has been no direct evidence indicating an in vivo interaction between Aip2p and actin cytoskeleton so far. Subsequently, the YDL178w gene product has been reported to localize on mitochondria and exhibit D-lactate dehydrogenase (DLD) activity in vitro, and therefore renamed as D-lactate dehydrogenase protein 2 (Dld2p) [1]. The AIP3 gene encodes actin interacting protein 3 (Aip3p), which is identical to BUD6 that functions in bipolar bud selection in yeast diploid cells [8–10]. Aip3p is not essential for mitotic growth but is necessary for normal morphogenesis, and plays an important role in actin-directed polarized cell growth in yeast cells.

We previously developed an in vitro protein conformation modifying assay that measures the factor-dependent increase in protease susceptibility of a substrate as a criterion for activity [11–13]. Serendipitously, we isolated a chaperone that alters the conformation of protein substrates such as F-actin in vitro. This purified chaperone is the Aip2p [1,3]. The activity of the isolated Aip2p could alter the conformation of F-actin in vitro and the rhodamine–phalloidin staining profiles as well as its osmotic sensitivity in vivo, which seems to be involved in yeast cell morphology.

Materials and methods

Yeast strains and antibodies. Wild-type yeast strains (ATCC24657 for the wild-type strain, ATCC96099 and ATCC 96100 were mated for the diploid cells) used in this study were purchased from American Type Culture Collection. Protease deficient strain SH2777 was a gift from Dr. Harashima, Osaka University. Anti-actin antibody was purchased from Chemicon. Anti-Aip2p antibody was raised against the synthetic peptide corresponding to the C-terminal 15 amino acid residues of Aip2p (VHYDPNGILNPYKYI) which were coupled through a COOH-terminal cysteine residue to BSA.

Purification of hexahistidine-tagged Aip2p. In an effort to obtain sufficient quantities of Aip2p, the protein was prepared from the expression strain in yeast under control of the ADH promoter. The C-terminally hexahistidine-tagged YDL178w gene was amplified by PCR and inserted into the aureobasidin A (Ab A) selective expression vector pAUR123 (TaKaRa Biomedicals). The protease deficient strain SH2777 was transformed by this plasmid and transformants were grown on YPD plates containing 0.5 μg ml^{-1} Ab A. Inoculated medium (8 L) was incubated overnight at 30 °C to an OD at 600 nm of 1–2. Cells were collected, resuspended in 4 volumes of buffer B (50 mM NaPi (pH 8.0), 150 mM NaCl, and 10 mM imidazole), crushed using glass beads, and centrifuged at 10,000 rpm for 10 min at 4 °C. Supernatants were collected and ultracentrifuged at 100,000*g* at 4 °C for 1 h. The precipitate was resuspended, passed through a Ni–NTA agarose column (Qiagen, K.K.) equilibrated in buffer B, and subsequently eluted with buffer B containing 0.5 M imidazole. Eluted fractions were dialyzed against buffer C (10 mM Hepes–KOH (pH 7.4), 50 mM NaCl, and 1 mM DTT), applied to an ion exchange Mono Q column (Amersham–Pharmacia Biotech, AKTA system) equilibrated with buffer C, and eluted with a linear NaCl gradient (100–500 mM). Immunoreactive fractions were dialyzed against buffer D (50 mM NaPi (pH 7.5), 10 mM NaCl, and 1 mM Mg $(OAc)_2$), and finally passed through a Superdex 200 gel filtration column equilibrated with buffer D.

Fluorescent microscopy. Rhodamine-labeled phalloidin (rhodamine–phalloidin) staining was performed as previously [14]. Samples were imaged with a Delta-Vision microscopy system (Applied Precision), with out of focus light pertaining to visualized images being removed by interactive deconvolution.

Formation of circular F-actin in vitro. Alexa 488-labeled G-actin (Molecular Probes) was converted into its Mg^{2+} form and polymerized for 2 h. Purified histidine-tagged Aip2p was added to Alexa 488-conjugated F-actin in the buffer E (10 mM Tris–Cl (pH 8.0), 0.1 M KCl, and 10 mM $MgCl_2$) and then incubated at 30 °C for 30 min in the presence of 1 mM ATP. Twenty microliter samples were then placed onto a glass-bottomed dish and covered with Slow fade anti-fade (Molecular Probes). To observe a staining profile of the circular F-actin with anti-Aip2p antibody, Alexa 594-conjugated anti-Aip2p antibody (red) was incubated with Alexa 488-conjugated F-actin (green). Affinity-purified Alexa 594-conjugated anti-Aip2p antibody was used at 1:100.

Trypsin susceptibility assay. Assays (200 μl) were initiated by adding 200 ng of polymerized rabbit muscle actin to buffer E containing 1 mM ATP and 500 ng of hexahistidine-tagged Aip2p, and incubated at 30 °C for 15 min. After incubation, samples were treated with trypsin (0.2 μg ml^{-1}) at 16 °C for 15 min. The reaction was terminated by incubation with soybean trypsin inhibitor (0.4 μg ml^{-1}) on ice for 5 min, TCA-precipitated with tRNA carrier, and then subjected to SDS–PAGE and Western blotting. To detect actin, affinity-purified polyclonal rabbit anti-actin antibody served as the primary antibody and horseradish peroxidase-linked IgG (ICN Pharmaceuticals) was the secondary antibody. Immunoreactive bands were visualized by ECL-plus (Amersham Biosciences) and analyzed using a Fluoro Smax (Bio-Rad).

Overexpression and disruption of actin interacting protein 2 gene in yeast cells. In an effort to obtain an Aip2p overexpressed strain, a cloned actin interacting protein 2 gene (AIP2) encoding Aip2p was inserted into the galactose inducible yeast expression vector pYES2. Yeast cells (ATCC96099) were transformed by this plasmid, selected on minimal plates without uracil, and checked by colony PCR. Aip2p was induced with 2% galactose at 30 °C for 6 h. To generate a strain containing a disrupted AIP2, the middle region of Aip2p (1039 base pairs) was substituted with a histidine marker gene fragment, and then inserted into pBluescript KS+ vector (Stratagene). A diploid strain was transformed with the linearized vector and the tetrads produced were then analyzed by Southern blotting to verify the presence of the disrupted gene.

Immunoprecipitation of Aip2p–actin complex. Yeast spheroplasts from wild-type or AIP2-deleted cells were gently homogenized in the buffer (10 mM Tris–Cl, pH 8.0, 0.1 M KCl, and 10 mM $MgCl_2$) followed by an centrifugation at 100,000*g* for 60 min at 4 °C. An antibody against the C-terminal peptide of Aip2p or an antibody against yeast actin (Chemicon) was conjugated to Formyl-cellulofine (Seikagaku-Kogyo) according to the manufacturer's instructions. The resin was equilibrated with immunoprecipitation buffer (20 mM Tris–HCl, pH 7.9, 75 mM KCl, 0.5 mM EDTA, 0.5 mM EGTA, and 8% sucrose) and then used for the immunoprecipitation.

Results

Aip2p–F-actin interaction in vitro

In the absence of Aip2p, polymerized F-actin displayed a linear structure (Fig. 1A, (−) Aip2p), whereas in the presence of Aip2p, de novo formation of circular F-actin was observed (Fig. 1A, (+) Aip2p). The average